Minerals Engineering 34 (2012) 55–62

Contents lists available at SciVerse ScienceDirect

Minerals Engineering

journal homepage: www.elsevier.com/locate/mineng

Unique challenges of clay binders in a pelletised chromite pre-reduction process

E.L.J. Kleynhans [a], J.P. Beukes [a,*], P.G. Van Zyl [a], P.H.I. Kestens [b], J.M. Langa [b]

[a] Chemical Resource Beneficiation, North-West University, Potchefstroom Campus, Private Bag X6001, Potchefstroom 2520, South Africa
[b] Xstrata Alloys Lydenburg Works, 1 Carrington Drive, Ohrigstad Road, Lydenburg 1120, South Africa

ARTICLE INFO

Article history:
Received 23 December 2011
Accepted 19 March 2012
Available online 15 May 2012

Keywords:
Chromite
Pre-reduction
Pelletisation
Clay binder
Bentonite
Attapulgite

ABSTRACT

Ferrochrome producers strive towards lower overall energy consumption due to increases in costs, efficiency and environmental pressures. In South Africa, in particular, higher electricity prices have placed pressure on ferrochrome producers. Pelletised chromite pre-reduction is most likely the ferrochrome production process option with the lowest specific electricity consumption currently applied. In this paper, the unique process considerations of clay binders in this process are highlighted and demonstrated utilising two case study clays. It is demonstrated that the clay binder has to impart high compressive and abrasion resistance strengths to the cured pellets in both oxidising and reducing environments (corresponding to the oxidised outer layer and pre-reduced core of industrially produced pellets), while ensuring adequate hot strength of pellets during the curing process. The possible effects of the clay binder selection and the amount of binder addition on the degree of chromite pre-reduction achieved were also investigated, since it could have substantial efficiency and economic implications. The case study results presented in this paper indicated that it is unlikely that the performance of a specific clay binder in this relatively complex process can be predicted, based only on the chemical, surface-chemical and mineralogical characterisation of the clay.

1. Introduction

Chromite ore mining is the only commercially viable source of new chromium units (Murthy et al., 2011; Beukes et al., 2010; Cramer et al., 2004). South Africa holds approximately 75% of the world's exploitable chromite resources (Basson et al., 2007; Cramer et al., 2004; Riekkola-Vanhanen, 1999), with other smaller but substantial deposits occurring in Kazakhstan, Zimbabwe, India and Finland (Papp, 2009). Approximately 90–95% of mined chromite is consumed by the metallurgical industry for the production of different grades of ferrochrome (FeCr). The stainless steel industry consumes 80–90% of FeCr, primarily as high-carbon or charge grade FeCr (Murthy et al., 2011; ICDA, 2010; Abubakre et al., 2007).

FeCr is produced largely by means of smelting chromite in submerged arc furnaces (SAFs) in the presence of carbonaceous reducing agents. Historically, the use of fine chromite (usually <6 mm) in this process is limited, since fine materials increase the tendency of the surface layer of the SAF to sinter. This traps evolving process gas, which can result in so-called bed turnovers or blowing of the furnace that could have disastrous consequences (Beukes et al., 2010; Riekkola-Vanhanen, 1999). The majority of chromite ore is relatively friable (Beukes et al., 2010; Glastonbury et al., 2010; Cramer et al., 2004; Gu and Wills, 1988); and therefore an agglomeration step is required (e.g. pelletisation), prior to feeding it into the SAF (Beukes et al., 2010; Singh and Rao, 2008).

South Africa is the leading producer of FeCr (ICDA, 2010). There are currently fourteen separate FeCr smelter plants in South Africa, with a combined production capacity of 4.7 million t/y (Beukes et al., accepted for publication; Jones, 2010). The abundant chromite resources and the relatively low historical cost of electricity have contributed to South Africa's dominant position (Basson et al., 2007). However, the electricity demand of South Africa has caught up with its electricity generating capacity. This has led to a dramatic increase in electricity prices that is set to continue in the foreseeable future (Basson et al., 2007). According to statistics from the National Energy Regulator of South Africa (NERSA) the nominal electricity price in South Africa increased steadily at a rate of roughly 0.58 RSA cents/kW h per year, in the period 1980 to 2005 (NERSA, 2009b). However, the nominal price of electricity has increased with 174% from 2007 to 2010 (NERSA, 2009a,b). NERSA has since granted Eskom, South Africa's sole electricity provider, a 3-year rate increase, resulting in electricity costs of 41.57 RSA cents/kW h for 2010/2011, 52.30 RSA cents/kW h for 2011/2012 and 65.85 RSA cents/kW h for 2012/2013 (Eskom, 2011; NERSA, 2009a). Considering that electricity consumption is the single largest cost component in FeCr production (Daavottila et al., 2004), the afore-mentioned cost increases are extremely significant. However, the pressure on South African FeCr producers is not unique, since globally lower specific energy consumption

* Corresponding author. Tel.: +27 82 460 0594; fax: +27 18 299 2350.
E-mail address: paul.beukes@nwu.ac.za (J.P. Beukes).

0892-6875
http://dx.doi.org/10.1016/j.mineng.2012.03.021

(MW h/t FeCr) and a decreased carbon footprint have become driving factors.

Historically, the specific energy consumption of conventional SAFs was 3.9–4.2 MW h/t FeCr (Naiker and Riley, 2006; Weber and Eric, 2006). Several processes have been developed to minimise energy consumption. However, the technology of interest in this study is the pre-reduction of chromite that is applied at two FeCr smelter plants in South Africa (Beukes et al., 2010; McCullough et al., 2010; Naiker, 2007; Naiker and Riley, 2006). In this process fine chromite ore, a clay binder and a carbon reductant are dry milled, pelletised and pre-heated before being fed into a rotary kiln where the chromite is partially pre-reduced. The pre-reduced pellets are then charged hot, immediately after exiting the kiln, into closed SAFs (Beukes et al., 2010; Naiker, 2007). The advantages of pelletised pre-reduction feed are observed in all aspects of operation, i.e. the ability to consume fine chromite; much lower specific energy consumption of approximately 2.4 MW h/t; chromium recoveries in the order of 90%, as well as the ability to produce a low silicon- and sulphur-containing FeCr product (McCullough et al., 2010; Naiker, 2007; Takano et al., 2007; Botha, 2003). It can therefore only be assumed that this process option will become more commonly applied as the pressure on energy consumption and environmental consciousness increases.

In the pelletised chromite pre-reduction process, clay is added to the raw material mixture to act as a binder for green (newly-formed) and cured strengths of the pelletised agglomerates. These functions are not unique, since clay binders also play a similar role in other chromite pelletisation processes. However, due to the unique nature of the pelletised chromite pre-reduction process, there are also aspects other than green and cured strength that should be considered during clay selection. In this paper, these unique process considerations of clay binders in the chromite pre-reduced process are highlighted and demonstrated utilising two clays for this case study.

2. Materials and methods

2.1. Materials

The raw materials utilised in the industrial pelletised chromite pre-reduction process consist of ore, a carbonaceous reducing agent and a clay binder. Raw material used in this study was obtained from a large South African FeCr producer, applying the pelletised chromite pre-reduction process. Samples of metallurgical grade chromite (<1 mm), anthracite breeze and two clays, i.e. attapulgite and bentonite utilised by this FeCr producer, were obtained.

Industrially produced pelletised chromite pre-reduced pellets were also obtained from the same FeCr producer. Industrial Analytical (Pty) Ltd. supplied SARM 8 and SARM 18 that were used as reference materials in the analysis of carbonaceous reductants and chromite containing materials, respectively. All other chemicals used were analytical grade (AR) reagents, obtained from the different suppliers and used without any further purification. Ultra-pure water (resistivity 18.2 MΩ cm^{-1}), produced by a Milli-Q water purification system, was used for all procedures requiring water. Instrument grade synthetic air and nitrogen gas were supplied by Afrox.

2.2. Methods

2.2.1. Chemical and surface analysis

Scanning electron microscopy with energy dispersive X-ray spectroscopy (SEM-EDS) was employed to visually and chemically characterise the surface properties of samples. Two different instruments were utilised, i.e. (i) a FEI QUANTA 200 ESEM, integrated with an OXFORD INCA X-Sight 200 EDS system operating with a 15 kV electron beam at a working distance of 10 mm and (ii) a Zeiss MA 15 SEM incorporating a Bruker AXS XFlash® 5010 Detector X-ray EDS system operating with a 20 kV electron beam at a working distance of 17.4 mm.

Inductively coupled plasma mass spectrometry (ICP-MS) and inductively coupled plasma optical emission spectrometry (ICP-OES) of the bentonite and attapulgite clays were performed. A Perkin Elmer Elan 6100 ICP-MS was utilised to determine minors and trace elements, while a Perkin Elmer Optima 5300 ICP-OES was used to characterise major components. ICP-OES of the metallurgical grade chromite ore, anthracite and the pre-reduced pellets was performed using a SPECTRO CIROS VISION ICP-OES Spectrometer.

Proximate (inherent moisture, ash, volatile matter and fixed carbon) analysis of the anthracite was performed according to the ASTM standard method D3172-07A (ASTM, 2007).

Elemental carbon and sulphur contents of the anthracite samples were determined by means of IR spectrophotometry utilising a LECO CS 244. A 1:1 mixture of tungsten and iron chips was used as the accelerator flux. Elemental carbon and sulphur analyses of the two clays were similarly conducted utilising a LECO CS 230 IR spectrophotometer. Additionally, the water loss and loss on ignition (LOI) of the clays were also determined at 110 and 1000 °C, respectively.

X-ray diffraction (XRD) of the clays was performed according to a back loading preparation method. Semi-quantitative and qualitative XRD analyses of the compounds in the clays were conducted with two different instruments, i.e. (i) a PANalytical X'Pert Pro powder diffractometer with Fe-filtered Co K radiation incorporating an X'Celerator detector and (ii) a Philips X-ray diffractometer (PW 3040/60 X'Pert Pro) with Cu Kα radiation. The measurements were carried out between variable divergence- and fixed receiving slits. The phases were identified using X'Pert Highscore plus software. The relative phase amounts were estimated using the Rietveld method (Autoquan programme).

2.2.2. Sample material preparation

A Wenman Williams & Co. disc mill was utilised to grind the lumpy attapulgite clay and the anthracite to <1 mm. Different mixing ratios of the three components present in the pre-reduced pellets (chromite ore, anthracite and clay) were then made up, according to the objectives of specific experiments. At the time of article preparation 3–4 wt.% clay addition was utilised in the industrial process. It was therefore decided to cover the 2.5–5 wt.% clay addition range. A 10 wt.% clay addition was also included to help identify trends that might be difficult to recognise at low clay additions. The anthracite was kept constant at 20 wt.% (relating to ~15 wt.% fixed carbon) in all experiments. The remainder of the mixtures were made up with the chromite ore.

All raw material mixtures were dry milled to the particle size specifications applied for industrial pre-reduction feed material (90% smaller than 75 μm). A Siebtechnik laboratory disc mill with a tungsten carbide grinding chamber, to avoid possible iron contamination, was used for this purpose. A Malvern Mastersizer 2000 was used to determine the particle size distribution of the pulverised material. A much diluted suspension of milled ore was ultrasonicated for 60 s prior to the particle size measurement, in order to disperse the individual particles without adding a chemical dispersant. It was determined that for a 50 g mixture of raw materials, a milling time of 2 min was required to obtain the desired size specification; therefore, all raw material mixtures were milled similarly.

2.2.3. Pelletising

The milled material was pressed into cylindrical pellets with an LRX Plus strength testing machine (Ametek Lloyd Instruments) equipped with a 5 kN load cell and a Specac PT No. 3000 13 mm die set. Pellets were prepared in batches of 10 each. For each batch 50 g of dry mixed raw material was pre-wetted with 5 g of water and mixed thoroughly. 3.2 g of pre-wetted material was then place in the die set and compressed at a rate of 10 mm/min until a load of 1500 N was reached, where after this load was held for 10 s. Although time consuming (each pellet made individually), this technique was preferred over conventional disc pelletisation, since disc pelletisation on laboratory scale can result in the formation of pellets with different densities, sizes and spherical shapes. The above described procedure ensured consistent density, form and size, which allowed the monovariance investigation of other process parameters.

2.2.4. Pre-reduction and oxidative sintering setup

A ceramic tube furnace (Lenton Elite, UK model TSH15/75/610) with a programmable temperature controller was used to conduct all pre-reduction and oxidative sintering experiments. Ceramic heat shields were inserted at both ends of the tube furnace to improve the tube length in which a stable working temperature could be achieved. These heat shields also protected the stainless steel caps, which were fitted onto both sides of the ceramic tube to seal the ends. The stainless steel caps had a gas inlet on the one side and an outlet on the other side.

The gaseous atmosphere inside the ceramic tube was controlled by either utilising a N_2 flow-rate of 1 NL/min, or a synthetic air-flow rate of 1 NL/min. N_2 was used during pre-reduction experiments, while synthetic air was used during oxidative sintering. An inert (N_2) gaseous atmosphere was preferred for the pre-reduction experiments, since pre-reduction caused by the carbonaceous reductant present in the material mixture was of interest in this study and not pre-reduction due to the presence of an external reducing gas. Before the pre-reduction experiments commenced, the tube furnace already loaded with pellets, was flushed with N_2 for at least 30 min at a flow rate of 1.25 NL/min at room temperature to remove oxidising gases.

Two furnace temperature profiles were used in this experimental study. These profiles were compiled in an attempt to simulate conditions occurring in the industrial pelletised pre-reduction of chromite. Both temperature profiles consisted of three segments, i.e. (i) heating up from room temperature to 900 °C over a period of 30 min, (ii) heating to the final temperature within a 50 min period (and soaking if applicable), and (iii) cooling down while gas flow was maintained. The first segments of both temperature profiles were identical, i.e. heating up to 900 °C in 30 min. In the second segment of the first temperature profile, the temperature was raised from 900 to 1250 °C within a 50 min period and held constant for 20 min, where after cooling down commenced. In the second segment of the second temperature profile, the temperature was raised from 900 to 1300 °C within a 50 min period, where after cooling started without any soaking time.

2.2.5. Compressive strengths testing

The compressive strengths of the pre-reduced or oxidative sintered pellets were tested with an Ametek Lloyd Instruments LRX-plus strength tester. The speed of the compression plates was maintained at 10 mm/min during crushing to apply an increasing force on the pellets. The maximum force applied to incur breakage was recorded for each pellet.

2.2.6. Abrasion resistance testing

The abrasion resistance test apparatus was based on a down-scaled version of the European standard EN 15051 rotating drum. The drum was designed according to specifications provided by Schneider and Jensen (2008). The drum was rotated at 44 rpm, which is faster than the rotating speed used by Schneider and Jensen (2008). This was done to obtain measurable abrasion on the hardest experimentally prepared pellets. A batch (ten pellets) of the pre-reduced or oxidative sintered pellets was abraded for the time periods 1, 2, 4, 8, 16 and 32 min. After every time interval, the material was screened using 9.5 and 1.18 mm screens. The over- and under-sized materials were then weighed and the material returned to the drum for further abrasion, until the final abrasion time was achieved.

2.2.7. Thermo-mechanical analysis (TMA)

Pellets were prepared in the same manner as described in Section 2.2.3, but not pre-reduced or oxidatively sintered as indicated in Section 2.2.4. A single pellet was placed in a Seiko Instruments Inc. TMA/SS 6100 thermo-mechanical analyser, interfaced with SII EXSTAR 6000. With this instrument, the thermal expansion of the pellet could be measured as a function of temperature up to 1300 °C. All TMA experiments were conducted in a N_2 atmosphere (1.67 NL/h), since oxidative corrosion of the internal parts of this specific instrument has been detected when operating under atmospheric gaseous conditions. Since the TMA probe was made of alumina, α-alumina coefficients correction was applied to the data, as specified in the operational manual of the instrument.

2.2.8. Ash fusion temperature analysis

Ash fusion temperature analysis is usually conducted to characterise the melting and sintering behaviours of coal ash (Nel et al., 2011). However, in this investigation it was applied to the two clays utilised as case study materials. The SABS ISO 540:2008 standard method was performed with a Carbolite CAF digital imaging coal ash fusion test furnace. In this test, a moulded cone of each clay was viewed and the following four temperatures recorded: (i) deformation temperature, when the corners of the mould first became rounded; (ii) softening temperature, when the top of the mould took on a spherical shape; (iii) hemisphere temperature, when the entire mould took on a hemisphere shape; and (iv) fluid temperature, when the molten material collapsed to a flattened button on the furnace floor.

2.2.9. Analysis of pre-reduction

The extent of chromite pre-reduction was determined according to the method utilised by laboratories associated with the FeCr smelters in South Africa currently applying the pelletised chromite pre-reduction process. The degree of pellet pre-reduction was determined using the following equation:

$$\%\text{Total Pre-reduction} = \frac{\frac{\%\text{Sol Cr}}{34.67} + \frac{\%\text{Sol Fe}}{55.85}}{0.0121}$$

The % Sol Cr and % Fe were determined by reflux leaching a fixed mass of the sample material with a hot sulphuric/phosphoric acid solution. The % Sol Cr in this aliquot was then established by oxidation of the soluble Cr with potassium permanganate and subsequent volumetric determination with ferrous ammonium sulphate using diphenylamine sulphonate as an indicator. The % Sol Fe in the aliquot (a portion not oxidised with potassium permanganate) was determined by a similar simple volumetric method, using potassium dichromate as the titrant and diphenylamine sulphonate as an indicator.

2.2.10. Statistical handling of data

The results reported were compiled from reiterations for every set of experimental conditions and procedures. Each compressive strength and abrasion resistance strength measurement reported was calculated from 20 and 3 repetitions, respectively. TMA and

pre-reduction analysis results were calculated from six and five reiterations for each set of experimental conditions. The mean and standard deviations were calculated for every dataset, after the elimination of possible outliers that were identified utilising the *Q*-test with 95% confidence level.

3. Results and discussion

3.1. Raw material characterisation

The chemical characterisation results of the raw materials utilised are indicated in Table 1. From these results, the Cr-to-Fe ratio of the chromite was calculated as 1.57, which is typical of South African deposits (Cramer et al., 2004; Howat, 1986). The anthracite had a fixed carbon content of approximately 75% and a volatile content of 6.87%. The major ash elements in the anthracite were found to be Si, Al, Fe, P, Ca and Mg. As expected, the clays were mainly alumina-silicates. The significance of other elements in the clays will be discussed later. Phosphorous and sulphur contents are usually included in the FeCr specifications (Basson et al., 2007); and therefore, they were also measured, where applicable.

3.2. Characterisation of typical industrial pellets

In order to illustrate the unique process considerations of clay binders in the pelletised chromite pre-reduced process, SEM backscatter micrograph images of an industrially produced pellet are shown in Fig. 1.

Fig. 1A is a partial micrograph of a polished sectional view taken at 45 times magnification of an industrial pre-reduced pellet split in half. It seems that there are two different zones in these pellets, i.e. the core and an outer layer, with a transitional zone in between. These two zones correspond to the different conditions to which the pelletised material is exposed during the industrial pre-reduction process. Initially, the raw material components (chromite, carbon reductant and clay) are homogeneously spread throughout the pellet. However, as the pellet is exposed to the high temperatures inside the rotary kiln, where the pre-reduction process takes place, the carbon in the outer layer is mostly burned off and a partially oxidised outer layer is formed at these high temperatures due to the presence of oxygen. A small amount of iron reduction can occur before all the carbon is consumed in this outer layer, which can be re-oxidised again. Oxygen ingress to the core does not take place, therefore the carbon in the core acts as a reductant resulting in pre-reduction without any oxidation impacting the core. Fig. 1B indicates the transitional area between these two different zones. In the core area (top right of Fig. 1B), small globules of pre-reduced metal can be seen, while the transitional zone (bottom left of Fig. 1B) seems to have a more sintered appearance without any significant metal globules. SEM-EDS analysis of the core and outer layer (not the transitional zone) revealed that the surface chemical carbon content of this specific pellet was approximately 7.1 wt.% in the core and approximately 1 wt.% in the outer layer. The small amount of carbon still present in the outer layer is most likely due to the formation of iron carbides, prior to complete oxidative combustion of free carbon in this layer. The thickness of the outer layer is usually less than 1 mm (approximately 0.5 mm in this

Table 1
Chemical characterisation of the different raw materials utilised with various analytical techniques.

Chromite			
ICP		EDS	
Cr_2O_3	45.37	Cr	27.21
FeO	25.39	Fe	15.33
Al_2O_3	15.21	Al	6.39
MgO	9.83	Mg	6.37
SiO_2	1.72	Si	3.70
CaO	0.22	Ca	0.48
P	<0.01	Ti	0.37
–	–	O	40.16

Anthracite			
ICP		EDS	
SiO_2	10.09	Si	2.53
Al_2O_3	3.13	Al	0.89
FeO	1.62	Fe	1.19
CaO	0.8	Ca	0.18
MgO	0.35	–	–
P	0.011	–	–
S	0.59	S	0.68
–	–	C	76.9
–	–	O	17.63
Proximate analysis			
FC		75.08	
Inherent Moisture		0.26	
Ash		17.79	
Volatiles		6.87	

Attapulgite			
ICP		EDS	
SiO_2	46.91	Si	21.80
Al_2O_3	14.76	Al	8.11
Fe_2O_3	6.72	Fe	5.32
Fe	4.70	–	–
CaO	5.63	Ca	3.14
MgO	5.29	Mg	2.91
TiO_2	0.26	Ti	0.15
–	–	Na	0.12
K_2O	0.21	K	0.09
MnO	0.15	–	–
P	<0.01	–	–
–	–	O	58.36
LECO			
C		1.47	
S		<0.001	
Water loss (110 °C)		8.73	
LOI (1000 °C)		13.04	

Bentonite			
ICP		EDS	
SiO_2	53.53	Si	23.61
Al_2O_3	13.17	Al	7.35
Fe_2O_3	5.33	Fe	5.73
Fe	3.73	–	–
CaO	4.77	Ca	3.37
MgO	2.64	Mg	1.70
TiO_2	0.45	Ti	0.31
–	–	Na	2.15
K_2O	1.14	K	1.10
MnO	0.08	–	–
P	0.02	–	–
–	–	O	54.69
LECO			
C		1.14	
S		<0.001	
Water loss (110 °C)		9.78	
LOI (1000 °C)		7.69	

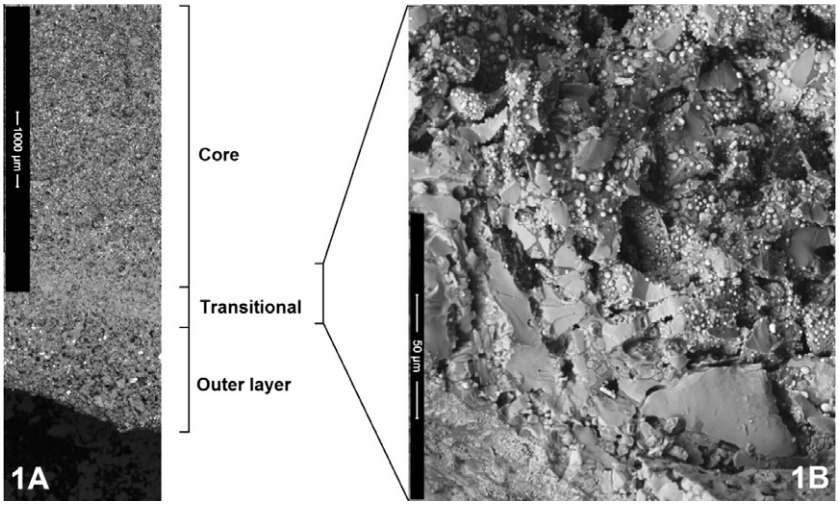

Fig. 1. SEM micrograph (45 times magnification) of a polished section of an industrial pre-reduced pellet split in half (1A), as well as a micrograph of an unpolished section zoomed in on the transitional zone, also showing part of the core area (1B).

case), while the overall diameter of the industrial pellets is usually between 12 and 20 mm.

From the above description, it is evident that the functioning of a clay binder within the pelletised chromite pre-reduced process has to be evaluated within two different environments, i.e. behaviour within an oxidative environment (corresponding to the outer layer of the industrially pre-reduced pellets) and behaviour within a reducing environment (corresponding to the core of the industrially pre-reduced pellets). This is in contrast with other chromite pelletised processes, e.g. the oxidative sintered pelletised process (Beukes et al., 2010) where only one condition prevails. In the paragraphs that follow, clay binder behaviour and characteristics are therefore explored in both environments (reducing and oxidative) in order to completely understand its functioning in the pelletised chromite pre-reduced process. In experiments where the oxidative sintering characteristics were investigated, the carbonaceous reducing agent, i.e. anthracite, was omitted from the raw material mixture to ensure that reducing behaviour did not influence the results.

3.3. Compressive strength

The compressive strength results for the pellets pre-reduced up to 1250 °C for 20 min (containing anthracite and pre-reduced under N_2), as well as oxidative sintered pellets cured at 1250 °C for 20 min (containing no anthracite and sintered in synthetic air) are shown Fig. 2. Fig. 3 shows similar results obtained with the second temperature profile utilised, i.e. maximum temperature of 1300 °C, with no soaking time.

From both these sets of results, several important deductions can be made. The compressive strengths of the oxidative sintered pellets were approximately an order of magnitude higher than that of the pre-reduced pellets. Therefore, although the objective of the industrially-applied pelletised chromite pre-reduced process is to achieve maximum pre-reduction, the compressive strength of pre-reduced chromite pellets is enhanced significantly by the thin oxidised outer layer (Section 3.2).

By comparison of the compressive strengths of the two case study clays, it is clear that the bentonite clay was superior in both pre-reducing and oxidative sintering environments. This is significant, since at the inception of this study, the attapulgite clay was the preferred option at both South African FeCr smelting plants applying the pelletised chromite pre-reduction process.

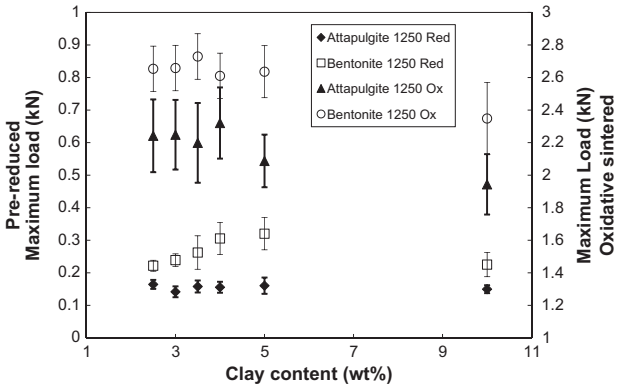

Fig. 2. Compressive strength (kN) of pre-reduced (primary axis) and oxidative sintered (secondary axis) pellets for the temperature profile up to 1250 °C and hold time of 20 min.

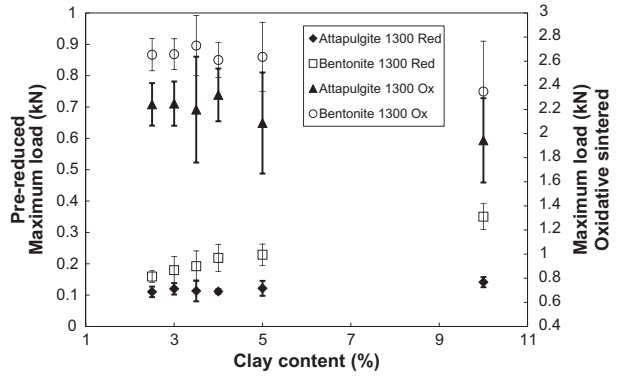

Fig. 3. Compressive strength (kN) of pre-reduced (primary axis) and oxidative sintered (secondary axis) pellets for the temperature profile up to 1300 °C with no hold time.

The compressive strength of the bentonite containing pre-reduced pellets generally improved with increased clay content between 2 and 5 wt.% additions, which is the industrially relevant addition range. Increased attapulgite content, however, did not result in any significant increase in compressive strength of the pre-reduced pellets. Increasing the attapulgite clay content of the

industrial pre-reduced pellets might therefore not result in a stronger pellet core (Section 3.2), although it might aid the green strength, which was not considered in this study.

For both clays used in this case study, larger clay additions resulted in a slight decreasing trend in compressive strengths of the oxidative sintered pellets. This indicates that clay content addition is not such an important parameter in attaining a strong oxidised outer layer (Section 3.2) on the industrially produced pellets.

3.4. Abrasion resistance

The abrasion resistance strength results for both pre-reduced and oxidative sintered pellets cured up to 1300 °C without holding time, for 3.5% and 10% clay contents, are shown in Fig. 4. The results are presented as the percentage weight retained in the size fraction >9.5 mm. Similar to the compressive strength results, the abrasion resistance strength of the oxidative sintered pellets was substantially better than that of the pre-reduced pellets for both clays. This again confirmed the importance of the oxidised outer layer (Section 3.2) in imparting strength to the industrially produced pellets. Furthermore, the bentonite outperformed the attapulgite in pre-reduced, as well as oxidative sintered abrasion resistance strength.

3.5. XRD and ash fusion temperature analysis

In order to explain the better performance of the bentonite compared to the attapulgite in compressive strength and abrasive resistance strength tests, SEM, SEM-EDS, XRD and ash fusion analyses were preformed. Visual inspection with SEM (e.g. observing bridge formations, pore sizes, densities, etc.) and chemical surface analysis with SEM-EDS did not provide any conclusive results and are therefore not discussed further.

Quantitative XRD analysis results of the two clays are presented in Table 2. Amorphous phases, if present, were not taken into account. In addition, mineral names may not reflect the actual compositions of minerals identified, but rather the mineral group. As expected, the smectite clay group minerals were the largest component in both clays. However, the attapulgite clay had considerably higher smectite group content than the bentonite. Considering only these results, the attapulgite clay may be mistakenly regarded as the better binder, due to the higher smectite mineral group content. Limitations of the Rietveld method prevent further breakdown of the smectite group, therefore qualitative XRD analyses were also conducted. Qualitative results indicated that the attapulgite contained palygroskite, which confirms its status as

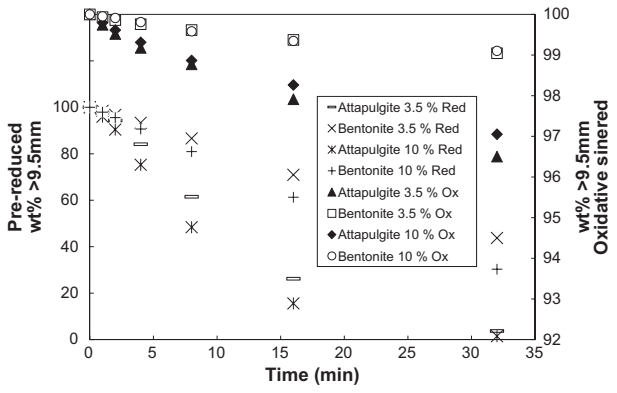

Fig. 4. Abrasion resistance strength indicated in weight percentage remaining above 9.5 mm versus abrasion time (note error bars were removed, since they were smaller than the markers).

Table 2
Quantitative XRD analysis of the attapulgite and bentonite clays utilised.

Attapulgite		Bentonite	
Augite	1.97	Augite	0.64
Calcite	6.66	Calcite	6.34
Kaolinite	2.45	Kaolinite	0.97
Muscovite	2.23	Muscovite	4.93
Orthoclase	1.78	Orthoclase	4.25
Plagioclase	3.86	Plagioclase	5.98
Quartz	4.22	Quartz	14.39
Smectite	76.8	Smectite	62.51

an attapulgite clay. In contrast the bentonite contained montmorillonite, but not palygroskite. It is therefore assumed that the aforementioned quantitative smectite mineral contents of the two clays can be ascribed to mainly palygroskite in the attapulgite and montmorillonite in the bentonite. However, trying to explain why the bentonite seems to be a better binder in the pellets, based only the above-mentioned mineralogical information would be presumptuous. Therefore, ash fusion tests were also conducted to derive parameters that maybe could clarify the previous observations (Sections 3.3 and 3.4). The four ash fusion temperatures recorded for each clay, both in oxidative and reducing conditions, are listed in Table 3.

The ash fusion temperatures indicated that the bentonite had lower deformation, softening, hemispherical and fluid temperatures in both oxidising and reducing environments, except for the initial deformation temperature in an oxidising environment. This can possibly give some practical explanation as to why the bentonite performed better in the compressive and abrasion resistance strength tests, for both pre-reduced and oxidative sintered pellets. A lower melting point (construed as incorporating all four measured ash fusion temperatures) implies that bentonite could possibly start forming bridges between the particles at lower temperatures than attapulgite. It is also notable that the fluid temperatures of the attapulgite in both environments were above 1300 °C, implying that that the possibility exists that it was not completely liquefied under the experimental conditions.

3.6. TMA analysis

Cold compressive and abrasion resistance strength tests give an indication of the cured strength of the pelletised materials after being treated in the different environments. However, the question could also be asked what the hot pellet strengths are, since that would influence pellet breakdown in the rotary kiln used in the industrial application. This has relevance to the formation or build-up of dam rings (material sticking to the inside of the rotary kiln). Unfortunately, no instruments that could directly measure high temperature compressive strength or abrasion resistance were available to the authors. A TMA instrument, which measures the thermal expansion of material as a function of temperature, was, however, available. TMA results for the pre-reduced pellets

Table 3
Ash fusion temperatures for the attapulgite and bentonite clays utilised.

Atmosphere	Ash fusion temperatures	Attapulgite	Bentonite
Reducing (N_2)	Initial deformation temperature	1216	1170
	Softening temperature	1242	1191
	Hemispherical temperature	1294	1251
	Fluid temperature	1337	1301
Oxidising (O_2)	Initial deformation temperature	1219	1224
	Softening temperature	1256	1255
	Hemispherical temperature	1336	1274
	Fluid temperature	1364	1304

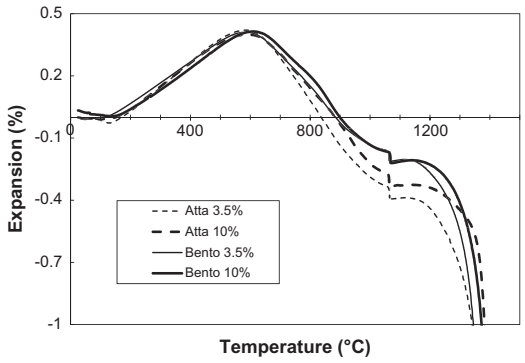

Fig. 5. Average percentage dimensional changes of *in situ* pre-reduction of pellets as a function of temperature for both clays investigated.

are shown in Fig. 5. Oxidative sintering could not be investigated due to instrumental limitation, as explained earlier (Section 2.2.7).

The TMA results of the pellets pre-reduced *in situ* containing either bentonite or attapulgite with the different clay wt.%, all indicate the same initial trends – small shrinkage up to about 120 °C that could probably be ascribed to moisture loss, followed by thermal expansion up to approximately 600 °C. After 700 °C, more significant shrinkage occurred for the attapulgite containing pellets. In the range 900–1200 °C, the attapulgite containing pellets had shrunk significantly more than the bentonite containing pellets did. This additional shrinkage of the attapulgite can possibly be related to the LOI of the attapulgite (13.04%) measured at 1000 °C (Table 1), which was significantly higher than the LOI of bentonite (7.69%). Although thermal expansion and shrinkage cannot be directly related to hot pellet strength, larger variation in thermal dimensional behaviour could possibly indicate weaker hot pellet strength. Therefore, although not quantitatively investigated, there is some indication that the hot strength of the attapulgite pellets could be weaker than the bentonite containing pellets.

3.7. Pellet pre-reduction

The amounts of pre-reduction achieved for the two temperature profiles used, as well as for clay contents from 2.5 to 10 wt.%, are shown in Fig. 6. There are a number of interesting features observed in this data. Firstly, the pre-reduction levels achieved with the 1250 °C temperature profile with holding times of 20 min were significantly higher than that achieved with the 1300 °C temperature profile without any holding time. According to the Ellingham diagram calculations of Niemelä et al. (2004), iron carbon reduction can occur above 710 °C, while chromium reduction is achieved

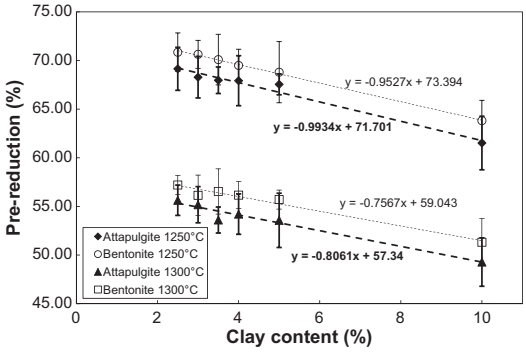

Fig. 6. Percentage pre-reduction achieved as function of clay content, for both case study clays and both temperature profiles utilised.

above 1200 °C. Therefore, the maximum temperature of the 1250 °C temperature profile was above temperatures required for both Fe and Cr reduction to occur and the higher levels of pre-reduction could be ascribed to the 20 min holding time.

From the data in Fig. 6, it is also evident that higher clay contents resulted in lower pre-reduction levels, for both clays and temperature profiles. This is significant within the industrial process, since higher clay contents are on occasion utilised to achieve improved green strength of the uncured pellets. In order to further quantify this observation, trend lines for the amount of pre-reduction with associated equations are given in Fig. 6. In the industrial application of pelletised chromite pre-reduction, clay contents between 3 and 4 wt.% are utilised. Substituting these values into the equations indicates that 0.76–0.99% lower pre-reduction levels can be expected if 4 wt.% instead of 3 wt.% clay addition is made. Not many references exist in the public domain that can be used to translate these lower pre-reduction values into energy and financial losses. Niayesh and Fletcher (1986) published a graph of chromite pre-reduction as a function of specific energy consumption (kW h/t FeCr produced), for different temperatures of pre-reduced feed material. The graph of Niayesh and Fletcher (1986), with the assumption that the material was fed into the furnace at room temperature, was reconstructed and an empirical fit of the data made. Using this fit and assuming 45% pre-reduction as the base case for an industrial plant, it was calculated that 16.7 kW h/t (for the 0.76% lower pre-reduction) to 21.7 kW h/t (for the 0.99% lower pre-reduction) more electricity would be used if 4 wt.% clay is added, instead of the 3 wt.%. This means that for a FeCr smelting plant producing 300 000 t/y, these values relate to 5006 to 6516 MW h/y more electricity, or ZAR2.62 to ZAR3.41 million calculated with the 52.30 RSA cent/kW h price of 2011/2012 (Eskom, 2011; NERSA, 2009c).

The third significant observation from the data in Fig. 6 is that there seems to be a difference between the performances of the two clays used in this case study with regard to pre-reduction levels achieved. Although some overlaps are observed between error bars, it is clear that the average pre-reduction of the bentonite containing pellets was consistently higher than that of the attapulgite containing pellets. Utilising intercept values on the *y*-axis of the trend lines, it was calculated that the bentonite containing pellets had an average of 1.7% higher chromite pre-reduction levels for both temperature profiles. This is significant, since this specific attapulgite clay was at the time of the inception of this study the preferred option at the South African FeCr smelters applying the pre-reduction process – this is primarily attributed to raw material cost considerations. By applying the fitted reconstructed plot of Niayesh and Fletcher (1986) as an indication, the difference in pre-reduction could also be converted to possible electricity and financial losses. For a 300,000 t/y smelter, operating at a specific energy consumption of 2.4 MW h/t, this relates to 9163–10 275 MW h/y more, or ZAR4.79 to ZAR5.37 million calculated with the 52.30 SA cent/kW h price of 2011/2012 (Eskom, 2011; NERSA, 2009c).

The reason for the better performance of the bentonite containing pellets with regard to pre-reduction could be attributed to two possible reasons, i.e. (i) the bentonite had a lower melting point (Section 3.5) than the attapulgite used in this case study, which may imply that the bentonite had already melted during the pre-reduction process, hence serves as a flux that promotes metal reduction, or (ii) the minerals present in the two clays can possibly contain materials that could either catalyse or inhibit the pre-reduction of chromite. Several studies have been published indicating that various substances could have catalytic or inhibiting effects on chromite pre-reduction (e.g. Takano et al., 2007; Weber and Eric, 2006, 1993; Ding and Warner, 1997a,b; Lekatou and Walker, 1997; Nunnington and Barcza, 1989; Van Deventer,

1988; Dawson and Edwards, 1986; Katayama et al., 1986). However, it is beyond the scope of this paper to deal specifically with possible differences in clay fluxing or catalytic and inhibiting clay effects.

4. Conclusions

The case study results presented in the paper proved that the clay binders utilised in the industrially applied pelletised chromite pre-reduction process have some unique process performance requirements that must be fulfilled. The clay binder has to impart high compressive and abrasion resistance strengths to the cured pellets in both oxidising and reducing environments (corresponding to the outer layer and the core of industrially produced pellets – Section 3.2). Without these characteristics, the pelletised material would break down, causing sintering on the surface of the SAF burden material and possible furnace eruptions. The hot pellet strength is equally important, since the breakdown of pellets that are pre-reduced in the rotary kiln results in the build-up of dam rings (material sticking to inside of kiln). While complying with the above-mentioned physical requirements, the clay binder must simultaneously not influence the pre-reduction of chromite negatively, since it could have significant consequences on electricity consumption during the smelting step. Testing of these unique process requirements on two study clays available to South African FeCr smelters applying the pre-reduction process, indicated that the previously preferred attapulgite clay is technically inferior in all aspects measured compared to the bentonite clay that is available as an alternative. Costs of these different clays were not considered in this study, which will obviously also influence the actual selection of clay used in the industry. It was also shown that higher clay content, e.g. to increase pellet green strength, will result in lower chromite pre-reduction. The case study results indicated that it is unlikely that the performance of a specific clay binder in this relatively complex process can be predicted based merely on the chemical, surface chemical and mineralogical characterisation of the clay. Experimental monovariance evaluation of clay performance on the characteristics identified in this study needs to be evaluated in order to distinguish which clay will be best suited for this unique process application.

Acknowledgements

The authors wish to thank Xstrata Alloys SA for financial support. Furthermore, Prof Quentin Campbell and Prof Marthie Coetzee are acknowledged for the use of the particle size analyser and the pulveriser, respectively.

References

Abubakre, O.K., Murian, R.A., Nwokike, P.N., 2007. Characterization and beneficiation of Anka chromite ore using magnetic separation process. Journal of Minerals & Materials Characterization & Engineering 6 (2), 143–150.

ASTM, 2007. D3172-07A Standard Practice for Proximate Analysis of Coal and Coke. In American Society for Testing and Materials (ASTM). Book of Standards v 05.06-Gaseous Fuels; Coal and Coke, West Conshohocken, USA.

Basson, J., Curr, T.R., Gericke, W.A., 2007. South Africa's ferro alloy industry-present status and future outlook. In Proc. of the 11th International Ferro Alloys Conference. New Delhi, India, pp. 3–24.

Beukes, J.P., Dawson, N.F., Van Zyl, P.G., 2010. Theoretical and practical aspects of Cr(VI) in the South African ferrochrome industry. The Journal of the Southern African Institute of Mining and Metallurgy 110 (12), 743–750.

Beukes, J.P., Van Zyl, P.G., Ras, M., accepted for publication. Treatment of Cr(VI) containing wastes in the South African ferrochrome industry – a review of currently applied methods. The Journal of The Southern African Institute of Mining and Metallurgy.

Botha, W., 2003. Ferrochrome production through the SRC process at Xstrata, Lydenburg Works. Journal of the South African Institute of Mining and Metallurgy 103 (6), 373–389.

Cramer, L.A., Basson, J., Nelson, L.R., 2004. The impact of platinum production from UG2 ore on ferrochrome production in South Africa. The Journal of the South African Institute of Mining and Metallurgy 104 (9), 517–527.

Daavottila, J., Honkaniemi, M., Jonkinen, P., 2004. The transformation of ferrochromium smelting technologies during the last decades. The Journal of the South African Institute of Mining and Metallurgy, October, pp. 541–549.

Dawson, N.F., Edwards, R.I., 1986. Factors Affecting the Reduction Rate of Chromite. In Proc of the 4th International Ferro-alloys Congress, Sao Paulo, Brazil, pp. 105–113.

Ding, Y.L., Warner, N.A., 1997a. Catalytic reduction of carbon-chromite composite pellets by lime. Thermochimica Acta 292, 85–94.

Ding, L., Warner, N.A., 1997b. Reduction of carbon-chromite composite pellets with silica flux. Ironmaking and Steelmaking 24 (4), 283–287.

ESKOM. 2011. Eskom retail tariff adjustment for 2011/2012. <http://www.eskom.co.za/content/priceincrease2011.pdf> (accessed 13.10.11.).

Glastonbury, R.A., Van der Merwe, W., Beukes, J.P., Van Zyl, P.G., Lachmann, G., Steenkamp, C.J.H., Dawson, N.F., Stewart, H.M., 2010. Cr(VI) generation during sample preparation of solid samples – a chromite ore case study. Water SA 36 (1), 105–109.

Gu, F., Wills, B.A., 1988. Chromite – Mineralogy and Processing. Minerals Engineering 1 (3), 235–240.

Howat, D.D., 1986. Chromium in South Africa. Journal of the South African Institute of Mining and Metallurgy 86 (2), 37–50.

ICDA (International Chomium Development Association), 2010. Statistical Bulletin 2010 edition. France, Paris.

JONES, R., 2010. Pyrometallurgy in South Africa. <http://www.pyrometallurgy.co.za/PyroSA/index.htm> (accessed 3.03.11.).

Katayama, H.G., Tokuda, M., Ohtani, M., 1986. Promotion of the Carbothermic Reduction of Chromium Ore by the Addition of Borates. The Iron and Steel Institute of Japan 72 (10), 1513–1520.

Lekatou, A., Walker, R.D., 1997. Effect of SiO_2 addition on solid state reduction of chromite concentrates. Ironmaking and Steelmaking 24 (2), 133–143.

McCullough, S., Hockaday, S., Johnson, C., Barza, N.A., 2010. Pre-reduction and smelting characteristics of Kazakhstan ore samples. In: Proc of the 12th International Ferroalloys Congress. Helsinki: Outotec Oyj. pp. 249–262.

Murthy, Y.R., tripathy, S.K., Kumar, C.R., 2011. Chrome ore beneficiation challenges & opportunities – a review. Minerals Engineering 24 (5), 375–380.

Naiker, O., 2007. The development and advantages of Xstrata's Premus Process. In: Proc. of the 11th International Ferroalloys Congress. New Delhi, India. pp. 112–119.

Naiker, O., Riley, T., 2006. Xstrata alloys in profile. In Southern African Pyrometallurgy 2006 Conference. Johannesburg, South Africa: South African Institute of Mining and Metallurgy. pp. 297–306.

Nel, M.V., Sstrydom, C.A., Schobert, H.H., Beukes, J.P., Bunt, J.R., 2011. Comparison of sintering and compressive strength tendencies of a model coal mineral mixture heat-treated in inert and oxidizing atmospheres. Fuel Processing Technology 92 (5), 1042–1051.

NERSA. 2009a. Eskom price increase application 2009. <http://www.nersa.org.za/Admin/Document/Editor/file/Electricity/PricingandTariffs/Eskom%20Current%20Price%202009-10.pdf> (accessed 8.09.11.).

NERSA. 2009b. Historic Eskom Average Selling Price. <http://www.nersa.org.za/Admin/Document/Editor/file/Electricity/PricingandTariffs/Eskom%20Historic%20Prices.pdf> (accessed 8.09.11.).

NERSA. 2009c. Inductive Future Eskom Price Direction. <http://www.nersa.org.za/Admin/Document/Editor/file/Electricity/PricingandTariffs/Eskom%20Future%20Pricepath.pdf> (access 8.09.11.).

Niayesh, M.J., Fletcher, G.W., 1986. An assessment of Smelting Reduction Processes in the Production of Fe–Cr–C Alloys. In: Proc. of the 4th International Ferro-alloys Congress. Sao Paulo, Brazil. pp. 115–123.

Niemelä, P., Krogerus, H., Oikarinen, P., 2004. Formation, characterization and utilization of CO-gas formed in ferrochrome smelting. In: Proc. of the 12th International Ferroalloys Congress. Cape Town, South, Africa. pp. 68–77.

Nunnington, R.C., Barcza, N.A., 1989. Pre-reduction of fluxed chromite-ore pellets under oxidizing conditions. In: Proc. of the 5th International Ferroalloys Congress. New Orleans, USA. pp. 55–68.

Papp, J.F., 2009. 2009 Minerals Yearbook Chromium [Advance Release]. <http://minerals.usgs.gov/minerals/pubs/commodity/chromium/myb1-2009-chrom.pdf> (accessed 19.10.11.).

Riekkola-Vanhanen, M., 1999. Finnish expert report on best available techniques in ferrochromium production. Helsinki.

Schneider, T., Jensen, K.A., 2008. Combined single-drop and rotating drum dustiness test of fine to nanosize powders. Annals of Occupational Hygiene 52 (1), 23–34.

Singh, V., Rao, S.M., 2008. Study the effect of chromite ore properties on pelletisation process. International Journal of Mineral Processing 88, 13–17.

Takano, C., Zambrano, A.P., Nogueira, A.E.A., Mourao, M.B., Iguchi, Y., 2007. Chromites reduction reaction mechanisms in carbon–chromites composite agglomerates at 1 773 K. Iron and Steel Institute of Japan International 47 (11), 1585–1589.

Van Deventer, J.S.J., 1988. The effect of additives on the reduction of chromite by graphite. Thermochimica Acta 127, 25–35.

Weber, P., Eric, R.H., 1993. The reduction mechanism of chromite in the presence of a silica flux. Metallurgical Transactions B 24B, 987–995.

Weber, P., Eric, R.H., 2006. The reduction of chromite in the presence of silica flux. Minerals Engineering 19, 318–324.